This is a postprint version of the following published document:

Ureña, J., Tabares, E., Tsipas, S., Jiménez-Morales, A., Gordo, E. (2019). Dry sliding wear behaviour of β-type Ti-Nb and Ti-Mo surfaces designed by diffusion treatments for biomedical applications. *Journal of the Mechanical Behavior of Biomedical Materials*, v. 91, March 2019, pp. 335-344.

Dry sliding wear behaviour of β-type Ti-Nb and Ti-Mo surfaces designed by diffusion treatments for biomedical applications

J. Ureña [1], E. Tabares [1], S. Tsipas [1, 2], A. Jiménez-Morales [1, 2], E. Gordo [1, 2]

[1]UNIVERSITY CARLOS III OF MADRID, Department of Materials Science and Engineering, IAAB, Avda. Universidad, 30, 28911 Leganés, Spain.
jurena@pa.uc3m.es; stsipas@ing.uc3m.es; toni@ing.uc3m.es; elena.gordo@uc3m.es

[2]ALVARO ALONSO BARBA TECHNOLOGICAL INSTITUTE OF CHEMISTRY AND MATERIALS, University Carlos III of Madrid

Abstract

The dry sliding wear behaviour of different Ti-Nb and Ti-Mo surfaces was investigated in order to evaluate the role of Nb and Mo β-stabilizing elements in titanium wear resistance to consider them for biomedical applications. Dry sliding wear tests were performed under unlubricated conditions using a ball-on-plate tribometer (UMT) with reciprocating lineal movement of 1 Hz frequency at different loads (2 and 5 N) and against two counterface materials (alumina and stainless steel) to assess the effect of these parameters on wear.
The results indicated an improvement in wear resistance for all the modified Ti surfaces. Metal-on-metal surfaces exhibited higher wear rate than ceramic-on-metal, and higher wear was observed for the more severe conditions. Wear rate values on modified surfaces were between 53-96 % lower compared to pure Ti tested at 2 N, and up to 79 % lower than Ti at 5 N. In both cases the highest wear reduction was observed for Ti-Mo$_{NH4Cl}$ surface.

KEYWORDS: β-gradient Titanium; Diffusion Treatments; Mo; Nb; Wear; Powder Technology.

1. Introduction

Recently, β-titanium alloys are increasingly being investigated due to their enhanced mechanical performance, high corrosion resistance and suitable biocompatibility ideal for knee and hip implants [1]. However they are no exempt from wear with the subsequent wear debris formation and metallic ion release to the surrounding biological tissues [2]. Titanium presents poor tribological behaviour due to low abrasive wear resistance, and this is an important factor in the failure of orthopedic joint implants [3], [4]. Thus, many of hip or knee joints studies focus on the wear of the femoral head against the acetabular cup employing different materials in order to solve the wear related problem, since the wear behaviour is highly dependent on materials, displacement, load and velocity [5]. The wear mechanisms identified in orthopedic implants are abrasive, adhesive, fatigue, fretting or corrosion, depending on numerous and interconnected factors including the material composition, surface properties, hardness and corrosion resistance [6]. Therefore, as it has been reported that bearing Ti surfaces can influence the bone-implant interface due to the poor wear resistance, many works are dedicated to wear protection of pure Ti and Ti alloys via different surface modification processes to enhance the hardness and abrasive wear resistance [3], [7], [8], [6]. Ion implantation, PVD coatings, plasma spray coatings, thermal oxidation,

carburization or boriding, or thermal treatments such as diffusion, nitriding or hardening are among the most used surface modification techniques for wear improvement [3], [9]. However, diffusion-based surfaces like those reported in this article are less common and the understanding of the wear behaviour is necessary in order to compare them to the currently used CP-Ti and Ti6Al4V alloys.

On the other hand, Nb is found to be beneficial to enhance the wear resistance of Ti because of its Nb_2O_5 passive layer which repassivates earlier and seems to stay longer than those passive layers with V or Al [4], [5], [10]. In that sense, Nb and Mo are employed in this study to create multifunctional surfaces with improved wear behavior and bioactivity, maintaining or enhancing corrosion resistance and providing lower Young's modulus without reducing material strength.

Recent investigations have been reported with similar strategies for wear improvement. Mo alloying in Ti6Al4V resulted in higher hardness and wear rate reduction [11]. There is evidence that a Ti-Nb layer deposited by double-glow plasma technology led to reduction in wear rate compared to pure titanium and improved the corrosion resistance [7]. However, the dry sliding wear behaviour of the superelastic Ti10V2Fe3Al alloy was studied at different load conditions; showing wear improvement at loads lower than 2 N while higher wear rates with loads superior to 2 N. Moreover, a relationship between wear mechanism and load was found, since loads lower than 2 N resulted mainly in oxidation whereas at higher loads the titanium alloy exhibited more tendency to adhesion [12]. Another important issue since implants are placed inside the body surrounded by biological fluid, both wear and tribocorrosion behaviour were evaluated for a β-Ti alloy used in femoral stems fabrication (Ti12Mo6Zr2Fe) and compared to that of the α+β Ti6Al4V alloy. The generation of unacceptable levels of wear debris due to hydroxyapatite particles formation during immersion in SBF, led to three-body abrasive wear deteriorating their tribocorrosion properties [13]. On the other hand regarding hardness, higher surface hardness is expected to be more wear resistant because of lower plastic deformation, lack of delamination and reduced wear volume. This was confirmed by a series of TixNb7Fe alloys, where abrasion and oxidation were the wear mechanisms observed (similarly to those of the employed CP-Ti), and where the hardest surface displayed superior wear resistance [14]. A wear rate reduction was also found for Ti5Al5Mo5V1Cr1Fe alloy after nitriding or thermal oxidation process [15]. In this work the thermo-reactive diffusion treatment is used as another way of wear improvement due to a nitriding process that takes place on surface during the reaction by the presence of an activating agent [16].

Therefore, this study is a contribution to fully evaluate the wear response of low elastic modulus and improved hardness β Ti-Nb and Ti-Mo surfaces in order to determine their potential for orthopedic applications since their bioactivity and cell behaviour have been already evaluated obtaining positive results [17], [18]. Hence, an extensive wear study of a series of Ti-Nb and Ti-Mo surfaces designed with microstructural β / α+β / α gradient or nitride porous surface processed through powder metallurgy has been carried out evaluating the effect of counter material, load and stroke length on their wear behaviour comparing it to titanium wear resistance.

2. Experimental procedure

2.1 Materials and sample preparation

A series of Ti-Nb and Ti-Mo surfaces were designed and fabricated by surface modification of Ti substrates produced from hydride-dehydride (HDH) commercially

pure titanium powder (CP-Ti grade 4) (GfE Metalle und Materialien GmbH, Germany) with mean particle size of 45 μm. The Ti substrates were fabricated by uniaxial pressing at 600 MPa and sintering in high vacuum (10^{-5} mbar) at 1250 °C for two hours with a heating and cooling rate of 5 °C/min [19].

Surface modification was carried out by thermochemical treatments to promote diffusion and/or thermo-reactions on the substrate surface. As diffusion elements, micro-sized Nb (1-5 μm) and Mo (1-2 μm) powders were used, and diluted aqueous suspensions were prepared and deposited by spraying [20] on the surfaces of sintered samples. Thermo-reactive treatment comprised of the inclusion of an activator (NH_4Cl) on the surface of the Ti substrates in addition to the Nb and Mo diffusion elements. As another via of diffusion treatment, the Nb suspension was also deposited onto green Ti substrates (as-pressed, before sintering) to investigate the effect of co-sintering on the final structures. The final surfaces were obtained after a thermal treatment at 1100 °C for 3 h in high vacuum (10^{-5} mbar) with heating/cooling at 5 °C /min and they were finished by a soft grinding step with a 1200# SiC emery paper. In the case of thermo-reactive diffusion a controlled Ar atmosphere was employed during the heat treatment. A schematic view of the material processing is given in Figure 1, summarizing diffusion elements, diffusion processes, final surface states and the nomenclature of the materials used in this study.

The samples were labelled according to the diffusion conditions. GreenTi-Nb makes reference to the Nb co-sintering + diffusion process in which the sample reached the surface modification in a single step during the thermal treatment in high vacuum (10^{-5} mbar). Ti-Nb and Ti-Mo refers to the Nb or Mo diffusion in a sintered Ti under high vacuum (10^{-5} mbar). Finally Ti-Nb$_{NH4Cl}$ and Ti-Mo$_{NH4Cl}$ refer to surface modification treatment through Nb or Mo thermo-reactive diffusion with the addition of an activator agent (NH_4Cl) in a controlled Ar atmosphere. The reference material was a polished sintered titanium substrate.
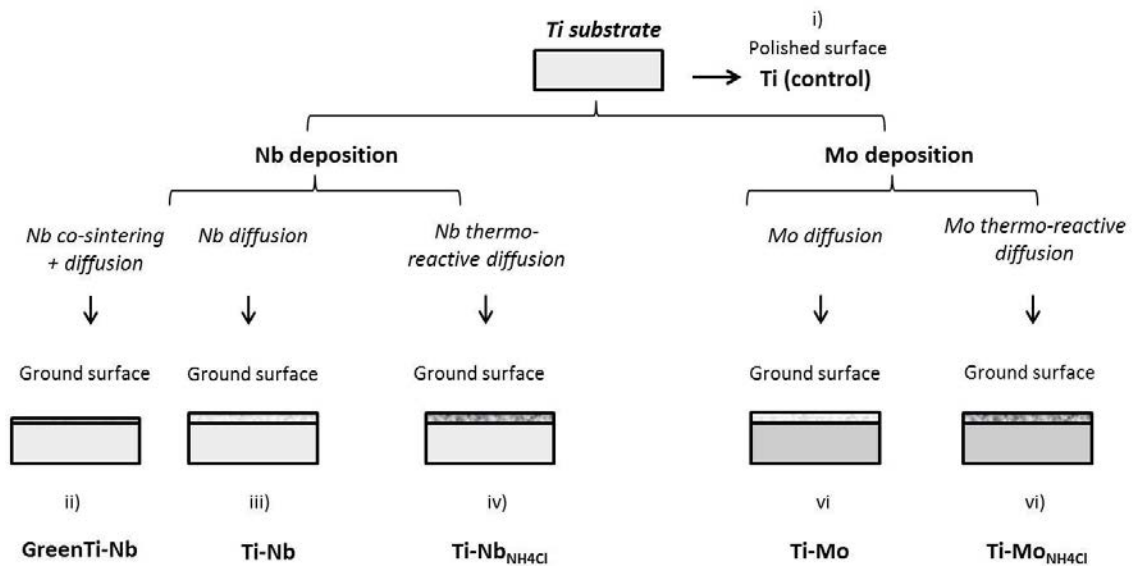

Figure 1. Scheme of the different β-type Ti-Nb and Ti-Mo surfaces designed.

2.2 Dry sliding wear tests

Dry sliding tests were performed on a ball-on-plate tribometer (UMT, Bruker) using reciprocating lineal movement. In the tests, the samples acted as the moving body

whereas the static body was the counter material. They were performed in ambient air under unlubricated conditions, and with purpose of comparison different conditions of counter material, load and amplitude were used since they have an important role on the tribological properties of materials [21], [22]. On one hand, the materials were tested by rubbing a 10 mm stainless steel ball under 2 N load, 1Hz frequency and 10 mm of total stroke length for 1800 s. On the other hand, a 6 mm alumina ball under 2 N and 5 N loads at 1 Hz frequency with a total stroke length of 10 and 5 mm, respectively, during 1800 s. All the conditions are summarized in Table 1. The tests were made in triplicate to obtain reliability in coefficient of friction (COF).

Parameters	*Setup [1]*	*Setup [2]*	*Setup [3]*
Load (N)	2	2	5
Counter material, Ball diameter (mm)	Stainless steel, 10	Alumina, 6	Alumina, 5
Stroke length (mm)	10	10	5
Frequency (Hz)	1	1	1
Sliding time (s)	1800	1800	1800

Table 1. Summary of the wear conditions tested together with the experimental scheme of the setup.

2.3 Wear rate

The wear tracks obtained from the dry sliding wear tests were measured in terms of width and depth by an optical profilometer (Olympus, DSX500, Opto-Digital Microscope). Three 2D profiles were taken from the middle (line 1), upper (line 2) and bottom part (line 3) of the wear track for each material (Figure 2). Before the calculation of the wear rate, the average depth (mm) and the volume loss (V) were obtained with the following parameters: $\bar{A}_w$ (average wear loss area of three 2D profiles in mm^2), $\bar{W}$ (average width of each track in mm), R (radius of the alumina ball; constant as 3 or 5 mm) and l (total stroke length; constant as 10 or 5 mm). Then, the wear rate, W_v, (in mm^3/mm) was calculated as the quotient of the volume loss, V, (in mm^3) between the total sliding distance (S) constant as 36000 or 18000 mm. For the calculation, the following formulas were used [23]:

$$\bar{D} = \bar{A}_w / \bar{W} \tag{1}$$

$$V = [1/3 * \pi * \bar{D} * (3R - \bar{D}) + (\bar{A}_w * l) \tag{2}$$
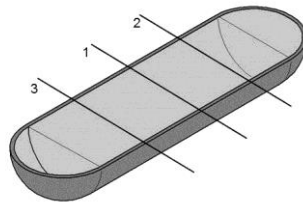
$$W_v = V/S \tag{3}$$

Figure 2. Model used for the wear loss volume calculation where line 1, 2 and 3 are the 2D profiles taken from the wear track of each material.

2.4 Microstructural characterization

A field emission scanning electron microscope FE-SEM (FEI, Teneo) equipped with EDAX, energy dispersive X-ray spectroscopy (EDS) was used to examine both the cross-section of all the materials to evaluate microstructure and phase transformation, as well as the worn surfaces after wear tests. Before and after wear evaluation, samples were ultrasonically cleaned in propanol for 10 min followed by distilled water for 5 min.

3. Results and discussion

3.1 Microstructure characterization

Figure 3 shows the microstructure of the modified Ti surfaces designed through Nb and Mo diffusion treatments. Based on the diffusion treatment applied (diffusion or thermo-reactive diffusion), two different types of microstructure are observed: i) β / α+β / α gradient of phases from surface to inward in the case of GreenTi-Nb, Ti-Nb and Ti-Mo; and ii) porous surface with a TiN layer created on surface in the case of Ti-Nb$_{NH4Cl}$ and Ti-Mo$_{NH4Cl}$. As seen from the SEM images, various depths of diffusion layers were obtained depending on the different mostly on the deposition treatment used. The diffusion layer of GreenTi-Nb, Ti-Nb and Ti-Mo showed a depth around 110-120 μm, consisting of a 30 μm β-phase region closer to surface corresponding to higher content in Nb or Mo plus a 80 μm α+β region with a decreasing Nb or Mo content, respectively. On the contrary, the diffusion layer of Ti-Nb$_{NH4Cl}$ and Ti-Mo$_{NH4Cl}$ exhibited a depth around 20-30 μm composed of a porous surface with the Nb or Mo remained on the surface together with a TiN layer originated by thermo-reactive diffusion due to the addition of the activating agent (NH$_4$Cl) which nitride the surface of these samples [16]. Mechanical properties of the modified Ti surfaces has previously been presented elsewhere [16], [24]. They showed an improved hardness of 4-5 GPa (twice the hardness of CP-Ti), where GreenTi-Nb, Ti-Nb and Ti-Mo exhibit a low elastic modulus between 53-64 GPa compared to 100-110 GPa of cp-Ti.
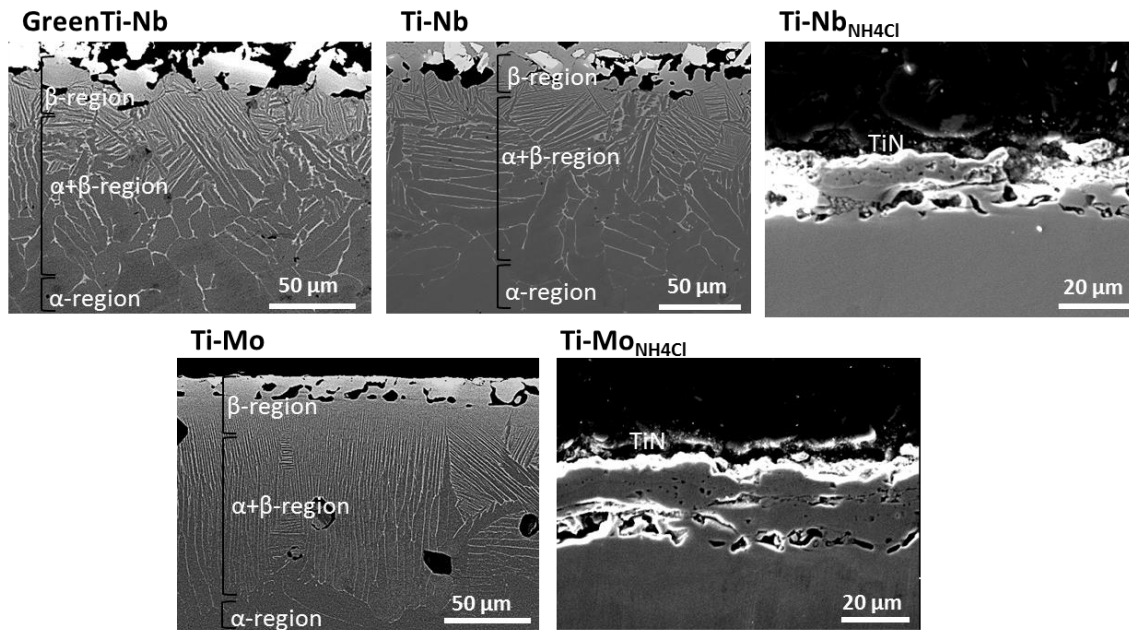
Figure 3. Cross-sectional SEM images of the modified Ti surfaces.

3.2 Dry sliding wear behaviour

The evolution of the coefficient of friction (COF) for all the samples during dry sliding wear tests according to setups from Table 1 is reported in Figure 4.

Friction test results between the modified Ti surfaces against stainless steel are given in Figure 4(a). Bare titanium exhibited a mean value of coefficient of friction around 0.45 with some oscillations reaching 0.7 at about 1400 s. These oscillations at the end of the test could be attributed to the large amount of particles detached from the material acting as third body [23] which can provoke an increase in wear loss volume and wear rate. A similar value was observed in GreenTi-Nb but showing a more stable coefficient of friction probably due to the introduction of niobium which is creating a more stable passive layer (Nb_2O_5) with good lubricant properties [5]. Moreover, the amount of iron detected by EDS analysis appears to be higher in Ti sample than in GreenTi-Nb, as indicated in Figure 5(e). This suggests less material transfer in GreenTi-Nb surface and it could be attributed to the fact that this passive layer repassivates more quickly. Moreover, results from EDS analysis (Figure 5e) suggest a reduction of the adhesive wear mechanism of all the surfaces compared to Ti.

COF values of Ti-Nb, Ti-Nb$_{NH4Cl}$ and Ti-Mo$_{NH4Cl}$ were much lower than Ti. They gradually increase throughout the rubbing action, remaining lower in the case of the Ti surfaces with Nb than in Ti-Mo$_{NH4Cl}$. The smoothest COF values were observed for Ti-Nb (0.15) and Ti-Nb$_{NH4Cl}$ (0.20) reaching a maximum value of 0.5 whereas Ti-Mo$_{NH4Cl}$ started with an initial value of 0.20 exhibiting a pronounced increase to 0.60. The more stable coefficient of friction of the modified Ti samples may be ascribed to lower debris formation which increases progressively. The β-surface of Ti-Nb sample seems to protect the material from the wear action lowering the friction value. However, the evolution of COF in Ti-Nb sample along time could be suggesting that the β-region is gradually worn and the α+β region of the sample is reached. In that sense, the evolution of COF could be associated to the change in microstructure. The first part of the wear test (lowest COF values) could match the rubbing action against the surface composed of β-phase while the second part (COF increase) could indicate the second layer of the

diffusion layer composed of α+β phases. This will be later discussed analyzing the depth of the wear tracks. In the case of the activated sample Ti-Mo$_{NH4Cl}$ (TiN surface) the COF increase could be attributed to higher wear debris formation since the examination of its worn surface (Figure 5d) did not show a significantly damaged surface.

On the other hand, friction test results between the modified Ti surfaces against alumina are given in figures 4(b, c). In general, the COF values from Figure 4(b) remain lower for longer times as compared to Figure 4(a) suggesting that the α+β region of the diffusion layers are reached later. This could be ascribed to lower friction and less wear debris formation since metal on metal produces higher friction due to adhesion mechanism than metal on ceramic [5]. The COF of Ti-Mo$_{NH4Cl}$ remains very low (0.1) and stable as compared to that obtained against stainless steel. The surface remained unaltered due to the hard nitride layer which seems to be practically not affected by the wear action. This behaviour was also found for a ion-nitrided Ti-10V-2Fe-3Al alloy and it was attributed to the compound layer formed which provokes no delamination wear mechanism [25]. Regarding COF of Ti-Nb and Ti-Mo surfaces, both of them showed similar values initially, increasing gradually from 0.1 to 0.5-0.6 coinciding with that of bare titanium. This increase in COF starts earlier in the Ti-Mo surface than in Ti-Nb (300 s and 1600 s, respectively). This suggests that the β-region is gradually worn in both materials and the abrasion mechanism reaches the steady state at these points when the coefficient of friction becomes until the end of the tests coinciding with the value of Ti. Moreover, it seems that the α+β region is reached earlier in Ti-Mo than in Ti-Nb, since the COF increases more rapidly in the former. Considering that the β-region depth is similar in both surfaces, the better friction behaviour of Ti-Nb could be explained due to the fact that Nb repassivates quickly and the Nb$_2$O$_5$ passive layer has an important lubrication effect [5]. Moreover, the stable COF values also could be related to the very little presence of Al found in EDS results (Figure 6f) which suggests the absence of adhesive wear.

In Figure 4(c), a similar COF behaviour could be observed for all the surfaces at short times. However, the COF increase is more pronounced for each sample compared to Figure 4(b). As it could be expected, a bigger load and shorter stroke length (5 N, 5 mm) had a significant effect on friction, and all modified surfaces reach earlier the COF of Ti. This means that the β-phase has a positive effect on the sliding wear behaviour and load bearing capacity of the material but it is affected by load conditions. This behaviour was also reported by [26] studying Ti-15Mo-xNb alloys under 1 N and 2 N load.

Although it is difficult to stablish a comparison with other investigations, similar conditions (4 N load and 8 mm stroke length) were used to evaluate a nitrided Ti-6Al-4V surface which resulted in COF values of 0.38-0.4 [27] similar to that obtained for this Ti-Nb$_{NH4Cl}$ surface. As seen from these results, it could be suggested that the surface modification employed by means of Nb and Mo diffusion and thermo-reactive diffusion (nitriding) have a positive effect lowering the friction between surfaces which also agrees with other related investigations where these elements are employed [7], [28].
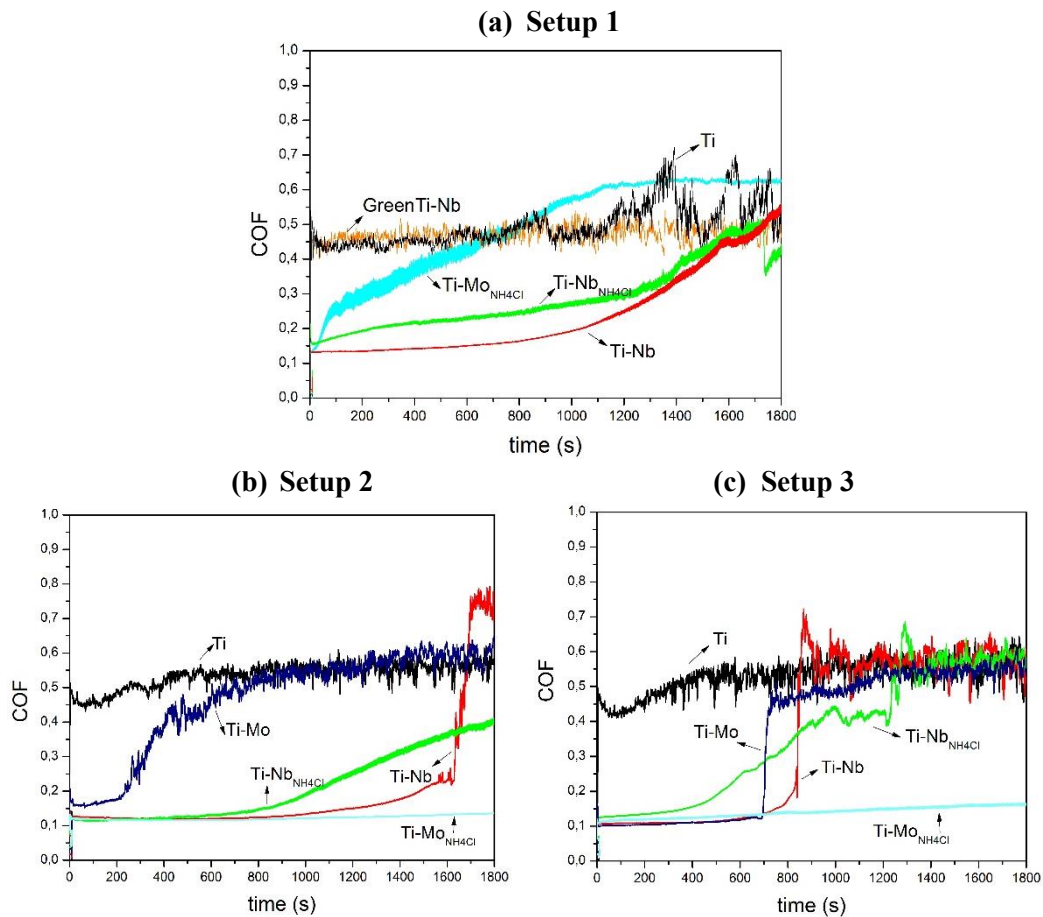
(a) Setup 1

(b) Setup 2

(c) Setup 3

Figure 4. Coefficient of friction (COF) during the dry sliding wear tests according to: (a) Setup 1 (2 N, 10 mm against stainless steel), (b) Setup 2 (2 N load, 10 mm against alumina) and (c) Setup 3 (5 N load, 5 mm against alumina).

Figure 5 illustrates general images of the worn surfaces showing the general aspect of wear tracks together with their higher magnification observations at 2 N load, 10mm stroke length against stainless steel. On one side, from the general view of the wear tracks, similar width tracks were detected for GreenTi-Nb and Ti-Nb which are slightly wider than Ti; but an important reduction of wear track width was found for Ti-Mo$_{NH4Cl}$ surface with a value of around 580 μm compared to 780 μm of Ti. On the other hand, examination of wear tracks shows the abrasive wear mechanism is dominant on Ti, GreenTi-Nb and Ti-Nb surfaces (Figure 5a-c) as evidenced by the parallel grooves. On the contrary, these are not observed in Ti-Mo$_{NH4Cl}$ (Figure 5d), where its structure remained unaltered which could be attributed to its higher surface hardness due to the nitride layer on surface. Apart from the grooves detected in SE, some dark areas are found in BSE images as indication of accumulated wear debris zones formed on Ti surface (Figure 5a). However, positively they were less evident in GreenTi-Nb and Ti-Nb (Figure 5b, c). EDS analysis (Figure 5e) taken from these areas revealed higher O and Fe content, indicating higher oxides formation in Ti that in all the modified Ti surfaces as well as higher Fe content as indication of adhesion wear. This type of wear mechanism is related to the adhesion between the surface atoms controlled by thermochemistry. Thus, the degree of adhesion can be determined by the mutual solubility of the materials [23]. Therefore, Fe seems to be more soluble in Ti than in Nb since Ti-Nb and GreenTi-Nb surfaces present lower Fe content compared to Ti (Figure

5e). Hence, a combination of abrasion, oxidation and adhesive wear seemed to be the wear mechanisms in Ti, while abrasion and oxidation wear dominate GreenTi-Nb and Ti-Nb surfaces. On the contrary, the Ti-Mo$_{NH4Cl}$ surface did not show grooves and its structure was not damaged. These results are in agreement with a similar investigation in which abrasion was reported as dominant wear mechanism in metal-on-metal friction and oxidation as wear mechanism at loads ≤ 2 N [12].
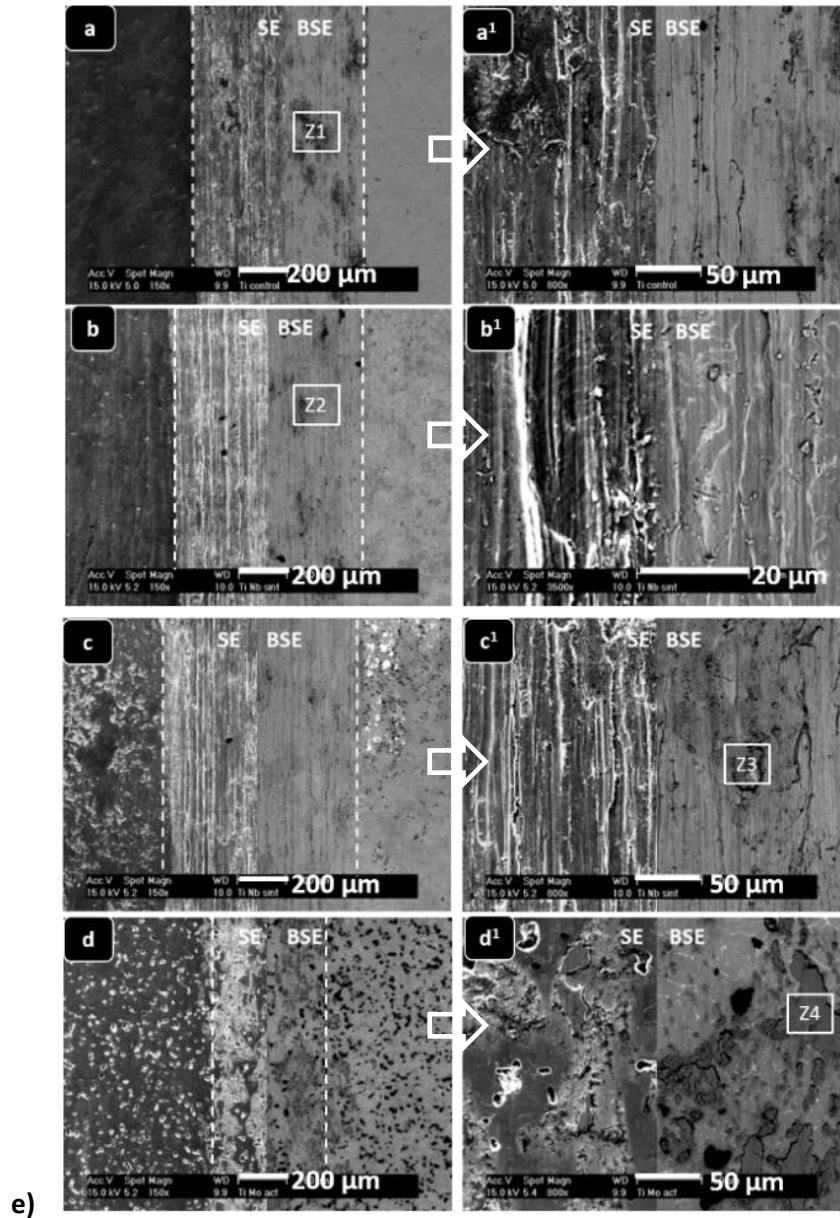

Figure 5. SE-BSE images of the wear tracks after dry sliding wear test at 2 N load, 10 mm against stainless steel (setup 1) on: a) Ti control, b) GreenTi-Nb, c) Ti-Nb and d) Ti-Mo$_{NH4Cl}$ surfaces. General view images on the left and higher magnification on the right. e) EDS values from selected areas.

Material	Areas	Ti [wt%]	O [wt%]	Fe [wt%]	Nb [wt%]	Mo [wt%]
Ti	Z1	71.7	30.6	7.6	-	-
GreenTi-Nb	Z2	69.3	17.4	3.5	9.7	-
Ti-Nb	Z3	68.3	16.7	3.2	11.9	-
Ti-Mo$_{NH4Cl}$	Z4	86.3	8.6	2.6	-	2.5

Figure 6 presents images of wear track together with an insert at lower magnifications at 2 N load, 10mm stroke length against alumina (Setup 2). A reduction of the wear track width was observed in all the modified Ti surfaces with respect to that of Ti. Ti-Mo$_{NH4Cl}$ presented the narrowest wear track followed by Ti-Mo and Ti-Nb$_{NH4Cl}$. As can be seen, Ti-Mo$_{NH4Cl}$ and Ti-Nb$_{NH4Cl}$ surfaces showed no damage on their structures. Thus, the thermo-reactive diffusion and consequently TiN deposition seems to reduce the damage of the material and only oxide formation can be detected as wear mechanism.

On the other hand, signs of abrasion wear grooves parallel to the sliding direction were found and clearly observed in Ti and Ti-Nb surfaces (Figure 6a, b) while in the rest of modified Ti surfaces they were less visible. Regarding EDS analysis (Figure 6f), a higher Al content was only detected in Ti and Ti-Mo surfaces. Thus, a combination of abrasion, oxidation and adhesive wear mechanism acted in the Ti surface, whereas oxidation and adhesion mechanisms in Ti-Mo. On the contrary, Ti-Nb surface only seemed to be affected by abrasion and oxidation. Compared to the metal on metal behaviour explained before at loads $\leq$ 2 N, alumina on Ti surfaces seems to reduce abrasion, while oxidation is the main wear mechanism.
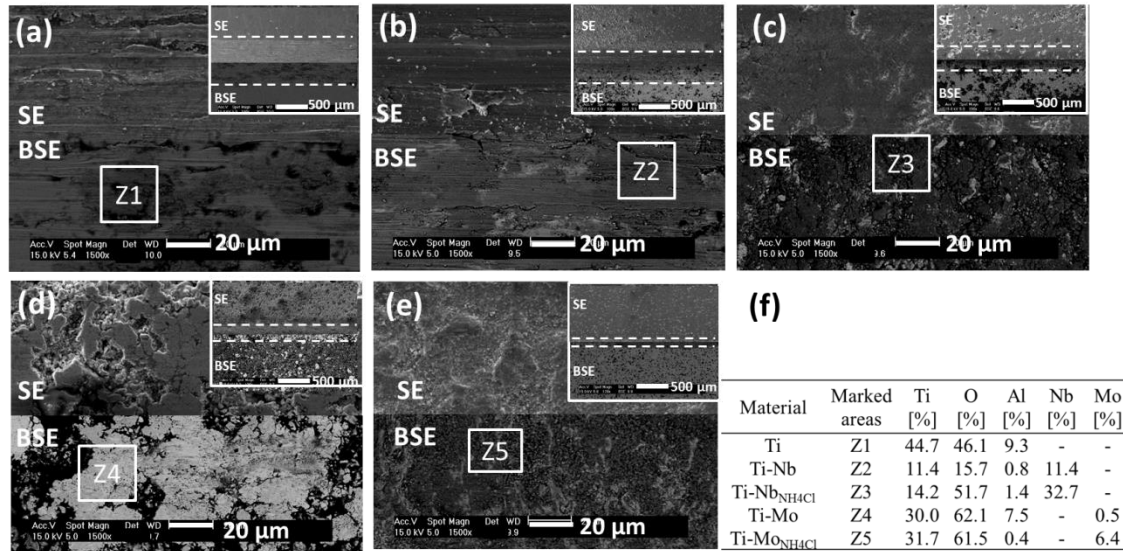

Figure 6. SE-BSE images of the wear tracks after dry sliding wear test at 2 N load, 10 mm against alumina (setup 2) on: a) Ti control, b) Ti-Nb, c) Ti-Nb$_{NH4Cl}$, d) Ti-Mo and e) Ti-Mo$_{NH4Cl}$ surfaces. General and detailed view images of the wear tracks. f) EDS values from selected areas.

Material	Marked areas	Ti [%]	O [%]	Al [%]	Nb [%]	Mo [%]
Ti	Z1	44.7	46.1	9.3	-	-
Ti-Nb	Z2	11.4	15.7	0.8	11.4	-
Ti-Nb$_{NH4Cl}$	Z3	14.2	51.7	1.4	32.7	-
Ti-Mo	Z4	30.0	62.1	7.5	-	0.5
Ti-Mo$_{NH4Cl}$	Z5	31.7	61.5	0.4	-	6.4

Figure 7 summarizes images of wear track and inserts at lower magnifications at 5 N load, 5mm stroke length against alumina (Setup 3). Similar information to ceramic on Ti surfaces at lower load can be drawn from these images. As expected, the effect of wear at higher load (5 N) was more severe and thus, a reduction of the wear track width in surface-treated samples was observed compared to Ti but this was less pronounced than the reduction obtained at 2 N load. Signs of severe abrasion were noticed in Ti, Ti-Nb and Ti-Nb$_{NH4Cl}$ where also some ridges may be produced by wear debris accumulation and material transfer that increased with respect to wear at 2 N suggesting also adhesive wear. Therefore, a combination of abrasion, oxidation and adhesion mechanisms is given for these surfaces against alumina when the applied load is 5 N.

This could indicate that the load increase from 2 N to 5 N led to a more severe wear with abrasion and adhesive mechanisms.

Similar dry sliding wear results were reported by [13] where at 5 N load and against alumina counterpart, adhesive was the main mechanism for the β-Ti alloy (Ti-12Mo-6Zr-2Fe) and a mixed mechanism of adhesion and abrasion on the Ti-6Al-4V alloy.
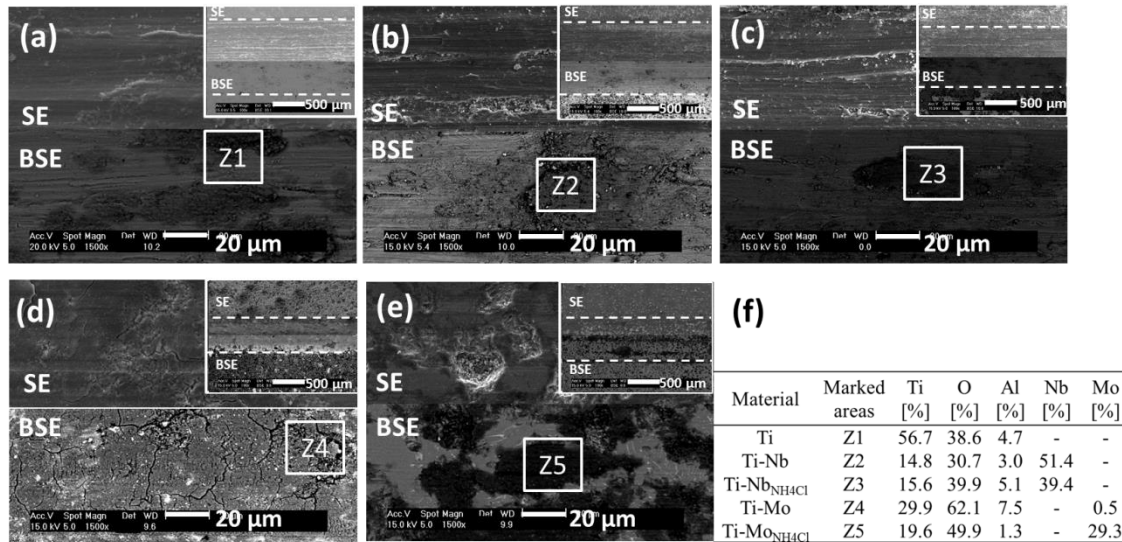

Figure 7. SE-BSE images of the wear tracks after dry sliding wear test at 5 N load, 5 mm against alumina (setup 3) on: a) Ti control, b) Ti-Nb, c) Ti-Nb$_{NH4Cl}$, d) Ti-Mo and e) Ti-Mo$_{NH4Cl}$ surfaces. General and detailed view images of the wear tracks. f) EDS values from selected areas.

Figure 8 shows the representative wear track profiles for the samples after dry sliding tests under different conditions. Profiles were taken from the center of the wear tracks, and the effect of load, stroke length and counter material on the wear behaviour of the modified Ti surfaces is discussed for the three setups selected.

First, from the comparison between Figure 8(a) and Figure 8(b), the effect of counter material on the total wear loss is presented. According to that reported by [5], metal on metal exhibits higher friction than on ceramic which is in agreement with our COF results (Figure 4) where higher coefficient of friction values where obtained for stainless steel on Ti surfaces, also confirmed by wear track profiles (Figure 8 a, b). Both conditions showed deeper wear tracks for Ti than for all the modified Ti surfaces. Metal on metal led to wear profiles with a maximum depth of 15 μm for Ti-Nb and 20 μm for GreenTi-Nb (Figure 8 (a)), which, considering the cross section of the samples (Figure 3) corresponds to the Nb-rich region (β-phase)/α+β region interface which explains the COF evolution and their increase when the α+β region is reached.

In the case of the activated material (Ti-Mo$_{NH4Cl}$) the surface displayed better wear resistance against a harder material such as alumina, exhibiting higher wear loss when it was rubbed against stainless steel. This may be ascribed to the lower wear debris formed by rubbing two harder materials (alumina on TiN) which produces less friction and increases the wear resistance of the material. COF values from Figure 4(b, c) suggested this behaviour since both nitride surfaces showed lower COF values against alumina counter material than against stainless steel. This confirms the surface hardening as one of the most effective techniques to improve wear resistance in Ti alloys as reported by [29].

Second, from Figure 8(b) and Figure 8(c) the effect of load and stroke length on wear track profile is discussed. As indicated in the COF graphs, COF values increased more quickly at 5 N than at 2 N. This COF behaviour suggested that the $\alpha+\beta$ region of the diffusion layers is reached earlier when a bigger load and a shorter stroke length are applied. As it was expected, the maximum depths of the wear track are less deep for the less severe conditions. The wear loss reduction for both nitrided surfaces (Ti-Mo$_{NH4Cl}$ and Ti-Nb$_{NH4Cl}$) and Ti-Mo is highly noticed in Figure 8(b) where the maximum wear profile is around 7 μm deep for all three of them compared to 20 μm for Ti. Regarding microstructure, this would correspond to the Mo-rich region (β-phase) in Ti-Mo material, and the nitride layer of the activated materials.

A very similar behaviour is shown for the surfaces in Figure 8(c). In this case, Ti-Nb and Ti-Mo showed maximum depths of 35 and 25 μm, respectively. In the cross-section, this depths correspond to the $\alpha+\beta$ region in both materials (Figure 3). These depths can be correlated to the change in COF behaviour indicating that $\alpha+\beta$ region is reached earlier compared to tests at 2 N load. Regarding nitride surfaces, Ti-Nb$_{NH4Cl}$ presented a maximum depth around 20 μm which corresponds to the diffusion layer in the cross-sectional microstructure (Figure 3) whereas Ti-Mo$_{NH4Cl}$ exhibited the lowest wear track depth of a maximum of 7 μm which remained in the nitride layer. This is in accordance with by the lower and stable COF behaviour shown by this material.

Therefore, under the three testing conditions, the wear tracks remained in the diffusion layers of the modified Ti samples. Specifically, in the microstructural (β / $\alpha+\beta$ / α) gradient, the maximum depth of the wear tracks reached the $\alpha+\beta$ region of the diffusion layers but not the α-area of the Ti substrate. This explained the COF evolution from lower to higher values, suggesting the partial removal of the β-area of the surfaces. This was more noticeable depending on the severity of the wear conditions: 2 N-ceramic was found to wear the least, 5 N-ceramic the most and 2 N-metal in-between both of them. Wear was less pronounced in the case of the hardest surfaces (Ti-Nb$_{NH4Cl}$ and Ti-Mo$_{NH4Cl}$) indicating superior wear resistance and an improvement of the load-bearing capacity.
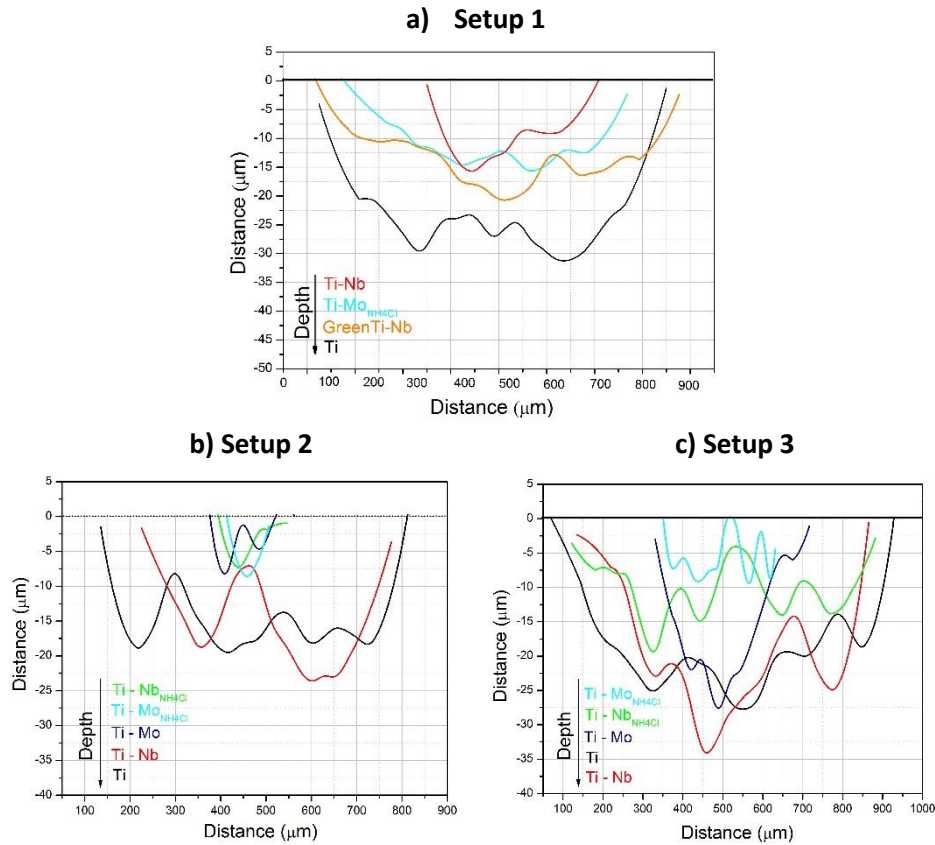
a) Setup 1

b) Setup 2

c) Setup 3

Figure 8. Wear track profiles for the modified Ti surfaces and Ti control material after dry sliding wear tests according to: a) Setup 1 (2 N, 10 mm against stainless steel), b) Setup 2 (2 N load, 10 mm against alumina) and c) Setup 3 (5 N load, 5 mm against alumina).

3D profile images of worn surfaces after wear testing against alumina are shown in Figure 9. Alumina was the counter material selected in order to evaluate the effect of load and stroke length (2 N-10 mm or 5 N-5 mm) on wear volume. This is an important issue in biomaterials since high wear volume is related to metallic ions release and adverse reactions in the body [5], [30].

Figure 9(a) corresponds to surfaces after 2 N load-10 mm stroke length (setup 2) while Figure 9(b) refers to 5 N load-5 mm stroke length (setup 3). In Figure 9(a), Ti surface exhibited a bigger and deeper wear track whereas Ti-Nb showed a smaller one. The rest of the surfaces practically remained unaltered which resulted in lower wear volume. The average wear volume obtained was around 6.8×10^{-2} mm^3, 3.2×10^{-2} mm^3, 7.5×10^{-3} mm^3, 7.3×10^{-3} mm^3 and 2.8×10^{-3} mm^3 for Ti, Ti-Nb, Ti-Nb$_{NH4Cl}$, Ti-Mo and Ti-Mo$_{NH4Cl}$, respectively.

A similar tendency was obtained for the more severe wear condition (Figure 9b). In this case the average wear volume remained around 8.03×10^{-2} mm^3, 7.22×10^{-2} mm^3, 4.49×10^{-2} mm^3, 2.63×10^{-2} mm^3 and 1.71×10^{-2} mm^3 for Ti, Ti-Nb, Ti-Nb$_{NH4Cl}$, Ti-Mo and Ti-Mo$_{NH4Cl}$, respectively.

In the end, Ti-Mo$_{NH4Cl}$ surface presented the minimum wear volume in both conditions. This is related to the high hardness due to the TiN layer of this treated-surface. On the other hand, a wear volume reduction was found in all the modified surfaces compared to Ti, but comparing Nb and Mo surfaces, the modification with Mo led to lower values of wear volume. This probably due to the Ti-Mo surface presents a slightly higher hardness value than Ti-Nb [24].
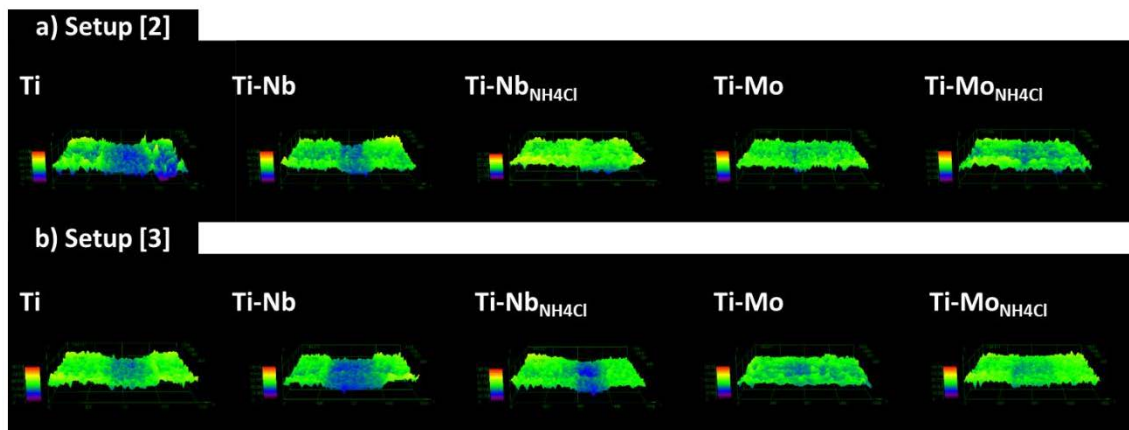
Figure 9. 3D profilometer images showing the wear tracks of all the surfaces after dry sliding tests at: a) setup2 (2 N load, 10 mm against alumina), and b) setup3 (5 N load, 5 mm against alumina).

The wear rate values after dry sliding tests under the different conditions are presented in Figure 10. Wear track profiles from Figure 8 suggested more wear in stainless steel on Ti surfaces than in alumina on Ti surfaces. This can be confirmed by the wear rate results mainly attributed to higher friction between metals. First, Figure 10(a) shows lower wear rates for the modified Ti surfaces than Ti. Wear rate of Ti-Nb and Ti-Mo$_{NH4Cl}$ was highly reduced (between 2-3 times less the value of Ti), while the value for GreenTi-Nb was similar to Ti.

On the other side, it is worth noticing the important decrease reached in all the modified Ti samples on wear rate when they are rubbed against alumina (Figure 10b). These values after 2 N load and 10 mm stroke length indicated a wear rate reduction of: 96 % (Ti-Mo$_{NH4Cl}$), 89 % (Ti-Nb$_{NH4Cl}$), 88 % (Ti-Mo) and 53 % (Ti-Nb) with respect to titanium. As it can be expected, wear became more evident at 5N load and shorter stroke length (setup 3). Thus, these values were relatively higher than those of setup 2 but with an important wear rate reduction compared to Ti: 79 % (Ti-Mo$_{NH4Cl}$), 67 % (Ti-Mo), 44 % (Ti-Nb$_{NH4Cl}$) and 10 % (Ti-Nb). Thereby, it can be considered that microstructure and composition; and thus hardness of titanium alloys play an important role on its wear behaviour. In this context, modified Ti surfaces composed of a gradient in microstructure (β / α+β) and composition (Ti-Nb or Ti-Mo) of these modified improves the wear resistance of bare titanium.
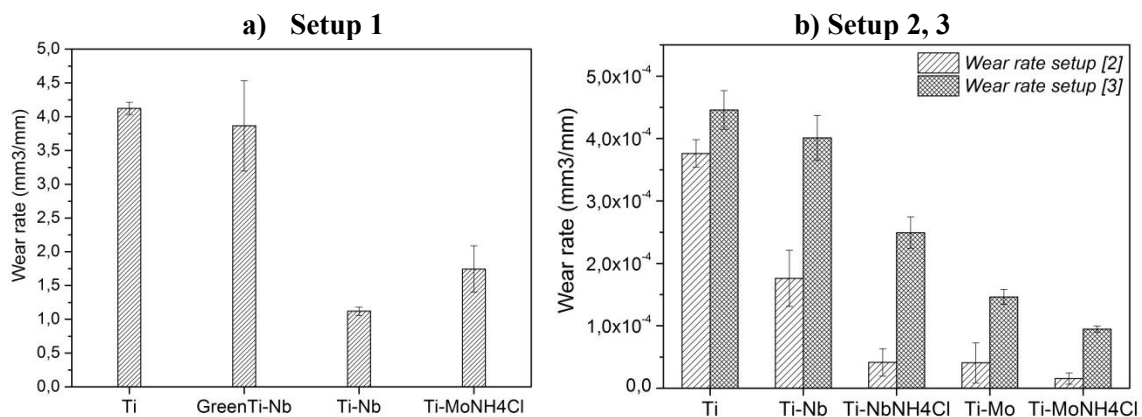
Figure 10. Wear rate values after dry sliding tests at 2 N load, 10 mm against stainless steel (setup 1); 2 N load, 10 mm against alumina (setup 2); and 5 N load, 5 mm against alumina (setup 3).

4. Conclusions

In this study, the dry sliding wear behaviour of different functionally gradient Ti-Nb and Ti-Mo surfaces composed of a microstructural gradient (β / α+β / α) was examined and compared to that of the (α-single phase) CP-Ti fabricated through powder metallurgy, exploring the effect of counter material, load and stroke length on their wear resistance. The main conclusions can be summarized as:

i) The modified Ti surfaces exhibited higher wear resistance compared to CP-Ti under all conditions, confirming the surface modification of titanium by niobium and molybdenum diffusion treatments as positive alternatives to improve the wear behaviour of Ti.

ii) Metal-on-metal (stainless steel on Ti surfaces) produced more signs of abrasion and adhesion wear, leading to higher wear rate than ceramic-on-metal (alumina on Ti surfaces).

iii) Comparing loads in ceramic-on-metal wear tests, wear rate was higher at 5 N load and 5 mm stroke length than at 2 N and 10 mm, indicating more signs of abrasion wear mechanism and material transfer due to more accumulation of wear debris.

iv) At 2 N load, the modified Ti surfaces showed wear rate values between 53-96 % lower compared to Ti. Similarly, at 5 N load they exhibited reduced values up to 79 % lower than bare Ti surface.

v) Ti-Mo$_{NH4Cl}$ surface indicated the highest wear reduction under all conditions respect to Ti wear resistance.

References

[1] Y. Li, C. Yang, H. Zhao, S. Qu, X. Li, and Y. Li, "New Developments of Ti-Based Alloys for Biomedical Applications," *Materials (Basel).*, vol. 7, no. 3, pp. 1709–1800, 2014.

[2] K. Apaza-bedoya, M. Tarce, C. A. M. Benfatti, B. Henriques, M. T. Mathew, W. Teughels, and J. C. M. Souza, "Synergistic interactions between corrosion and wear at based dental implant connections : A scoping review," *J. Periodontal Res.*, pp. 1–9, 2017.

[3] X. Liu, P. K. Chu, and C. Ding, "Surface modification of titanium, titanium

alloys, and related materials for biomedical applications," *Mater. Sci. Eng. R Reports*, vol. 47, no. 3–4, pp. 49–121, 2004.

[4]   M. Hussein, A. Mohammed, and N. Al-Aqeeli, "Wear Characteristics of Metallic Biomaterials: A Review," *Materials (Basel).*, vol. 8, no. 5, pp. 2749–2768, 2015.

[5]   M. Geetha, a. K. Singh, R. Asokamani, and a. K. Gogia, "Ti based biomaterials, the ultimate choice for orthopaedic implants - A review," *Prog. Mater. Sci.*, vol. 54, no. 3, pp. 397–425, 2009.

[6]   A. Revathi, S. Magesh, V. K. Balla, M. Das, A. Revathi, S. Magesh, V. K. Balla, and M. Das, "Current advances in enhancement of wear and corrosion resistance of titanium alloys – a review," *Mater. Technol. Adv. Perform. Mater.*, vol. 7857, pp. 1–9, 2016.

[7]   Q. Wang, P. Zhang, D. Wei, X. Chen, R. Wang, and H. Wang, "Microstructure and sliding wear behavior of pure titanium surface modified by double-glow plasma surface alloying with Nb," *Mater. Des.*, vol. 52, pp. 265–273, 2013.

[8]   H. Search, C. Journals, A. Contact, M. Iopscience, I. O. P. Conf, and I. P. Address, "Wear behavior of the plasma and thermal oxidized Ti-15Mo and Ti-6Al-4V alloys," *Mater. Sci. Eng.*, vol. 12055, no. 174, pp. 1–9, 2017.

[9]   M. A. Hussein, A. S. Mohammed, N. Al-aqeeli, and S. Arabia, "Wear Characteristics of Metallic Biomaterials: A Review," *Materials (Basel).*, vol. 8, pp. 2749–2768, 2015.

[10]   V. Goriainov, R. Cook, J. M. Latham, D. G. Dunlop, and R. O. C. Oreffo, "Bone and metal: An orthopaedic perspective on osseointegration of metals," *Acta Biomater.*, vol. 10, no. 10, pp. 4043–4057, 2014.

[11]   J. G. Tang, D. X. Liu, C. Bin Tang, X. H. Zhang, H. Xiong, and B. Tang, "Tribology behavior of double-glow discharge Mo layers on titanium alloy in aviation kerosene environment," *Trans. Nonferrous Met. Soc. China (English Ed.*, vol. 22, no. 8, pp. 1967–1974, 2012.

[12]   M. Mehdi, K. Farokhzadeh, and A. Edrisy, "Dry sliding wear behavior of superelastic Ti–10V–2Fe–3Al β-titanium alloy," *Wear*, vol. 350–351, pp. 10–20, 2016.

[13]   X. Yang and C. R. Hutchinson, "Corrosion-wear of beta-Ti alloy TMZF (Ti-12Mo-6Zr-2Fe) in simulated body fluid," *Acta Biomater.*, vol. 42, pp. 429–439, 2016.

[14]   S. Ehtemam-haghighi, K. G. Prashanth, H. Attar, A. K. Chaubey, G. H. Cao, and L. C. Zhang, "Evaluation of mechanical and wear properties of Ti-xNb-7Fe alloys designed for biomedical applications," *Mater. Des.*, vol. 111, pp. 592–599, 2016.

[15]   L. Liu, Y. J. Shangguan, H. Z. Li, H. B. Tang, and H. M. Wang, "Sliding wear behavior of laser-nitrided and thermal oxidation- treated Ti–5Al–5Mo–5V–1Cr–1Fe alloy fabricated by laser melting deposition," *Appl. Phys. A Mater. Process.*, no. 122:477, pp. 1–7, 2016.

[16]   S. A. Tsipas and E. Gordo, "Molybdeno-Aluminizing of Powder Metallurgy and Wrought Ti and Ti-6Al-4V alloys by Pack Cementation process," *Mater. Charact.*, vol. 118, pp. 494–504, 2016.

[17]   J. Ureña, S. A. Tsipas, A. Jiménez-Morales, E. Gordo, R. Detsch, and A. R.

Boccaccini, "In-vitro study of the bioactivity and cytotoxicity response of Ti surfaces modified by Nb and Mo diffusion treatments," *Surf. Coat. Technol.*, vol. accepted, 2017.

[18] J. Ureña, S. Tsipas, A. Jiménez-Morales, E. Gordo, R. Detsch, and A. R. Boccaccini, "Cellular behaviour of bone marrow stromal cells on modified Ti-Nb surfaces," *Mater. Des.*, vol. accepted, 2017.

[19] L. Bolzoni, T. Weissgaerber, B. Kieback, E. M. Ruiz-Navas, and E. Gordo, "Mechanical behaviour of pressed and sintered CP Ti and Ti-6Al-7Nb alloy obtained from master alloy addition powder," *J. Mech. Behav. Biomed. Mater.*, vol. 20, pp. 149–161, 2013.

[20] J. Ureña, C. Mendoza, B. Ferrari, Y. Castro, S. A. Tsipas, A. Jiménez-Morales, and E. Gordo, "Surface Modification of Powder Metallurgy Titanium by Colloidal Techniques and Diffusion Processes for Biomedical Applications," *Adv. Eng. Mater.*, vol. DOI: 10.10, pp. 1–8, 2016.

[21] G. Jin, B. S. Xu, H. D. Wang, Q. F. Li, and S. C. Wei, "Tribological properties of molybdenum coatings sprayed by electro-thermal explosion directional spraying," *Surf. Coatings Technol.*, vol. 201, no. 15, pp. 6678–6680, 2007.

[22] N. Diomidis, S. Mischler, N. S. More, and M. Roy, "Tribo-electrochemical characterization of metallic biomaterials for total joint replacement," *Acta Biomater.*, vol. 8, no. 2, pp. 852–859, 2012.

[23] Z. Doni, A. C. Alves, F. Toptan, J. R. Gomes, A. Ramalho, M. Buciumeanu, L. Palaghian, and F. S. Silva, "Dry sliding and tribocorrosion behaviour of hot pressed CoCrMo biomedical alloy as compared with the cast CoCrMo and Ti6Al4V alloys," *Mater. Des.*, vol. 52, pp. 47–57, 2013.

[24] J. Ureña, E. Tejado, J. Y. Pastor, F. Velasco, S. Tsipas, A. Jiménez-Morales, and E. Gordo, "Role of beta-stabilizer elements in microstructure and mechanical properties evolution of PM modified Ti surfaces designed for biomedical applications," *Euro PM 2017 Proceedings, ISBN 978-1-899072-49-1*, 2017.

[25] J. Qian, K. Farokhzadeh, and A. Edrisy, "Ion nitriding of a near-β titanium alloy: Microstructure and mechanical properties," *Surf. Coat. Technol.*, vol. 258, pp. 134–141, 2014.

[26] L. Xu, S. Xiao, J. Tian, and Y. Chen, "Microstructure , mechanical properties and dry wear resistance of β -type Ti−15Mo−x Nb alloys for biomedical applications," *Trans. Nonferrous Met. Soc. China*, vol. 23, no. 3, pp. 692–698, 2013.

[27] T. M. Manhabosco, S. M. Tamborim, C. B. dos Santos, and I. L. Müller, "Tribological, electrochemical and tribo-electrochemical characterization of bare and nitrided Ti6Al4V in simulated body fluid solution," *Corros. Sci.*, vol. 53, no. 5, pp. 1786–1793, 2011.

[28] A. Fan, Y. Ma, R. Yang, X. Zhang, and B. Tang, "Friction and wear behaviors of Mo-N modified Ti6Al4V alloy in Hanks' solution," *Surf. Coatings Technol.*, vol. 228, pp. S419–S423, 2013.

[29] M. Niinomi, "Mechanical biocompatibilities of titanium alloys for biomedical applications," *J. Mech. Behav. Biomed. Mater.*, vol. 1, no. 1, pp. 30–42, 2008.

[30] L. Kunčická, R. Kocich, and T. C. Lowe, "Advances in Metals and Alloys for Joint Replacement," *Prog. Mater. Sci.*, no. April, 2017.